◆ Human Brain Mapping 37:3835–3846 (2016) ◆

Abnormal Reward Circuitry in Anorexia Nervosa: A Longitudinal, Multimodal MRI Study

Jiook Cha,[1,2]* Jaime S. Ide,[3] F. Dubois Bowman,[4] Helen B. Simpson,[1,5] Jonathan Posner,[1,2] and Joanna E. Steinglass[1,5]*

[1]*Department of Psychiatry, Columbia University Medical Center, New York, New York*
[2]*Division of Child and Adolescent Psychiatry, New York State Psychiatric Institute, New York, New York*
[3]*Department of Biomedical Engineering, Stony Brook University, Stony Brook, New York*
[4]*Department of Biostatistics, Mailman School of Public Health, College of Physicians and Surgeons, Columbia University, New York, New York*
[5]*Division of Clinical Therapeutics, New York State Psychiatric Institute, New York, New York*

Abstract: Anorexia nervosa (AN) is a debilitating illness and existing interventions are only modestly effective. This study aimed to determine whether AN pathophysiology is associated with altered connections within fronto-accumbal circuitry subserving reward processing. Diffusion and resting-state functional MRI scans were collected in female inpatients with AN ($n = 22$) and healthy controls (HC; $n = 18$) between the ages of 16 and 25 years. Individuals with AN were scanned during the acute, underweight phase of the illness and again following inpatient weight restoration. HC were scanned twice over the same timeframe. Based on univariate and multivariate analyses of fronto-accumbal circuitry, underweight individuals with AN were found to have increased structural connectivity (diffusion probabilistic tractography), increased white matter anisotropy (tract-based spatial statistics), increased functional connectivity (seed-based correlation in resting-state fMRI), and altered effective connectivity (spectral dynamic causal modeling). Following weight restoration, fronto-accumbal structural connectivity continued to be abnormally increased bilaterally with large (partial $\eta^2 = 0.387$; right NAcc-OFC) and moderate (partial $\eta^2 = 0.197$; left NAcc-OFC) effect sizes. Increased structural connectivity within fronto-accumbal circuitry in the underweight state correlated with severity of eating disorder symptoms. Taken together, the findings from this longitudinal, multimodal neuroimaging study offer converging evidence of atypical fronto-accumbal circuitry in AN. *Hum Brain Mapp 37:3835–3846, 2016.* **© 2016 Wiley Periodicals, Inc.**

Key words: anorexia nervosa; corticostriatal connectivity; diffusion MRI; probabilistic tractography; resting state fMRI; spectral dynamic causal modeling; longitudinal study

Additional Supporting Information may be found in the online version of this article.

Contract grant sponsor: NIMH grants; Contract grant numbers: R21 MH099388 (JS & JP), K23 MH76195 (JS), and K23 MH091249 (JP); Contract grant sponsor: Klarman Family Foundation (JS); Contract grant sponsor: Brain and Behavior Research Foundation NARSAD Young Investigator Award (JC); Contract grant sponsor: Shire Pharmaceuticals (Dr. Posner).

*Correspondence to: Joanna Steinglass, MD; New York State Psychiatric Institute, Room 2406 Unit: 98, 1051 Riverside Dr. New York, NY 10032. E-mail: js1124@cumc.columbia.edu OR Jiook Cha, PhD; New York State Psychiatric Institute, Room 2420 Unit: 74, 1051 Riverside Dr. New York, NY 10032.
E-mail: chajioo@nyspi.columbia.edu
Jonathan Posner and Joanna Steinglass equally contributed to this work.

The authors declare no competing financial interests.

Received for publication 18 January 2016; Revised 18 April 2016; Accepted 20 May 2016.

DOI: 10.1002/hbm.23279
Published online 8 June 2016 in Wiley Online Library (wileyonlinelibrary.com).

INTRODUCTION

Anorexia nervosa (AN) is a serious mental illness with a mortality rate among the highest of any psychiatric disorder [Arcelus et al., 2011]. Although the neural underpinnings of AN remain unknown, both reward processing and the associated neural circuits are thought to be disturbed among individuals with the disorder [Kaye et al., 2009; O'Hara et al., 2015]. Food, for example, is typically considered a primary reward, yet for individuals with AN the subjective experience of food and eating is extremely complex. This clinical phenomenon highlights the importance of investigating the structure and function of reward circuitry in AN.

Prior studies have investigated neural correlates of reward processing in AN. Structural MRI studies have shown volumetric abnormalities among individuals with AN within reward-sensitive regions, including the orbitofrontal cortex (OFC) and caudate nucleus in acutely ill individuals with AN and recovered individuals, although the direction of these abnormalities (increased vs. decreased volumes) have been inconsistent [Frank et al., 2013a; Titova et al., 2013]. Task-based fMRI studies have shown abnormal striatal and prefrontal cortex activity in response to monetary stimuli (in AN before and after weight restoration [Decker et al., 2015] and in recovered AN [Wagner et al., 2007]). Abnormal task-related responses have also been shown, with increased Blood-Oxygenation-Level-Dependent (BOLD) activity within the OFC and nucleus accumbens (NAcc) in both acutely ill individuals with AN [Fladung et al., 2010] and individuals recovered from AN [Cowdrey et al., 2011]. A positron emission tomography (PET) study in recovered AN indicated increased dopamine receptor density in the NAcc [Frank et al., 2005], although this finding was not replicated in a more recent study with larger samples of acute AN [Broft et al., 2015]. Across this range of neuroimaging modalities and study designs, the findings suggest atypical reward circuitry in AN.

The NAcc has the major afferent projections from the orbitofrontal cortex and the ventromedial PFC [Haber and Knutson, 2010]. Since this projection is crucial to reward processing and decision making, an abnormal connection, for example, abnormally increased intrinsic functional connectivity, is often implicated in various psychiatric disorders, such as OCD [Graybiel and Rauch, 2000]. Given the shared symptoms between OCD and AN, abnormally heightened connectivity may also explain the pathophysiology of AN; however, no such prior reports exist.

Advances in neuroscience have led to an emphasis on neural circuits, rather than isolated brain regions, as putative mechanisms of psychopathology [Insel, 2009]. Neural connectivity assessments include a range of sophisticated methodologies for characterizing neural circuits. Diffusion MRI (dMRI) examines the diffusion of water molecules and can index tissue architecture and the orientation of white matter fibers [Mori and Zhang, 2006]. Resting-state functional MRI identifies correlations in spontaneous fluctuation of BOLD signals. Spectral Dynamic Causal Modeling (spDCM) builds on this approach and uses a Bayesian framework to estimate effective connectivity, based on neurophysiological modeling of the BOLD signal. In doing so, spDCM provides estimates of the direction of neural interactions and neurobiological characteristics (e.g., excitatory or inhibitory connections) underlying dynamics of such interactions [Razi et al., 2015].

We aimed to examine the fronto-accumbal connectivity of in AN using multiple methods of analysis. To investigate brain circuit abnormalities that are not alleviated by refeeding, we aimed to evaluate this circuitry longitudinally by obtaining MRI scans from patients before and after weight restoration. We hypothesized that relative to healthy controls (HC), individuals with AN, before and after weight restoration, would demonstrate aberrant fronto-accumbal connectivity. The novelty of this research impeded specific hypotheses about the direction of this effect. Using spDCM and structural equation modeling (SEM), we also explored neurobiological aspects of the fronto-accumbal connection in AN and common factors (i.e., latent variables) underlying multiple connectivity measures across modalities and analyses that are associated with AN.

MATERIALS AND METHODS

Participants

Individuals in this study were enrolled in a functional neuroimaging study of AN [Decker et al., 2015] and participated in additional MRI scanning procedures, as described below. Participants were unmedicated individuals with AN ($n = 22$) receiving inpatient treatment at the New York State Psychiatric Institute (NYSPI) and HC ($n = 18$). Patients with AN were female, 16–25 years old, and met DSM-5 criteria for AN (12 restricting subtype and 10 binge-purge subtype) at the time of hospital admission and study enrollment (Table I). Treatment at NYSPI is a behaviorally based program focused on weight restoration [Attia and Walsh, 2009]. Patients begin treatment with a prescribed 1,800 kcal diet for the first week. Study procedures began within the first week of hospitalization for medically stable patients; this assured that patients had received at least 24 hours of nourishment prior to participation. Diagnosis was made by Structured Clinical Interview for DSM-IV (SCID) [Goodman et al., 1989] and the Eating Disorder Examination (EDE) [Cooper and Fairburn, 1987]; patients without amenorrhea were included, consistent with DSM 5 diagnostic criteria. Participants (including HC) had no contraindications to MRI, and were not taking psychotropic medication at the time of MRI scanning. Individuals were excluded if they had an estimated IQ less than 80 (determined by Wechsler Test of Adult Reading; [Wechsler, 2001], history of a neurological, bipolar, or

TABLE I. Demographic and clinical characteristics of participants

	AN (Mean, SD)	HC (Mean, SD)	Statistics (t or χ^2)	P (2-sided)
Ethnicity	C, 20; AA/H, 1; As, 1	C, 12; AA/H, 4; As, 2	$\chi^2 = 3.77$	0.15
Time 1	$n = 22$	$n = 18$	–	–
Age (years)	19.5 (2.42)	20.5 (2.95)	$t = 1.04$	0.30
BMI (kg/m^2)	17.3 (1.24)*	21.2 (1.63)	$t = 8.28$	<0.001
DE-Q	3.9 (1.37)	0.1 (0.13)	$t = 11.89$	<0.001
Education (years)	13.3 (1.83)	13.9 (2.4)	$t = 0.86$	0.39
Estimated IQ (WTAR)	104.2 (8.28)	107.9 (12.13)	$t = 1.08$	0.29
Time 2	$n = 19$	$n = 15$	–	–
Days between sessions	47.6 (10.13)	49.2 (29.51)	$t = 0.21$	0.83
BMI(kg/m^2)	20.0 (0.47)	21.4 (1.76)	$t = 3.25$	0.003
EDE-Q	2.4 (1.56)	–	$t = 4.11^{\dagger}$	<0.001

*At scanning, range, 14.8 (min)-19.01 (max); BMI at admission was lower: mean, 16.3 (1.37); range, 12.5 (min)-18.2 (max).
†Paired t-tests within AN between Time 1 and 2.
AA/H, African American/Hispanic; As, Asian; C, Caucasian; WTAR, Wechsler Test of Adult Reading, Eating Disorder Examination-Self-Report Questionnaire Version.

psychotic disorder, substance abuse in the last 6 months, or if they were pregnant. Anxiety or depressive disorders, which commonly co-occur with AN [Hudson et al., 2007], were not exclusionary, as long as AN was the primary diagnosis (one person had comorbid dysthymia; two had major depressive disorder; and three had specific phobia).

HC were group-matched for age, sex, and ethnicity and were included if they had no current or lifetime psychiatric illness, no significant medical illness and had a BMI in the normal range (18.0–25.0 kg/m^2). This study was approved by the NYSPI Institutional Review Board, and after complete description of the study, adult participants provided written informed consent; adolescent participants provided assent with a parent/guardian providing consent (ClinicalTrials.gov NCT00325520).

Procedures

For individuals with AN, study procedures were completed within one week of hospital admission[1] (Session 1), and then again after weight restoration to a BMI of at least 19.5 kg/m^2 for 2 weeks (Session 2). Time between scanning sessions was group-matched for AN and HC (43 ± 12 days vs. 51 ± 31 days; $t = 1.047$, $P = 0.31$). At the time of each MRI session, participants were administered the Eating Disorder Examination Self-Report Questionnaire (EDE-Q) [Fairburn and Beglin, 1994].

[1]For three individuals who were more severely underweight at the time of admission, medical stabilization (as determined by the clinical team, independent of the research staff) required a longer duration of medical stabilization prior to participation in neuroimaging procedures (mean duration of 20 ± 12.4 days).

MRI Data Acquisition

Images were acquired on a 1.5 T Philips Intera scanner with an 8-channel head coil. Each session consisted of structural, diffusion, and resting-state functional MRI. Acquisition of T1-weighted sagittal localizing images was followed by a 3D spoiled gradient recall (SPGR) image (TR = 25 sec, TE = 3.7 ms, flip angle = 30°, FOV = 256 mm, 256 × 204 matrix, 128 slices, voxel size 1 × 1 × 1 mm). Two runs of dMRI were collected (TR = 10,586 ms, TE = 70 ms, 70 slices, voxel size = 2 × 2 × 2 mm, skip = 0). The diffusion series included two initial images acquired without diffusion weighting and with diffusion weighting along 16 non-collinear directions ($b = 800$ sm^{-2}). For resting fMRI image acquisition, participants were instructed to stay still with their eyes open, and to let their minds wander freely. Two 5-minute resting fMRI sessions were obtained (TR = 2,000 ms, TE = 40 ms, flip angle = 77°, 33 Slices, voxel size = 3 × 3 × 3 mm, 150 volumes). Some individuals did not complete rs-fMRI because of time constraints.

MRI Preprocessing and Analysis

Overview

We assessed structural and functional aspects of fronto-accumbal connectivity in AN. Our primary assay of structural connectivity was probabilistic diffusion tractography. The connection strength or the likelihood of two regions (seed and target) being connected via white matter tracts, was estimated. A secondary, voxel-wise analysis of diffusion anisotropy measures (e.g., fractional anisotropy) was carried out using Tract-Based Spatial Statistics. For functional connectivity, we performed seed-based correlation analysis using an accumbal seed. Based on the functional connectivity findings, we lastly investigated potential

neuronal circuit mechanisms underlying abnormal intrinsic functional connectivity in AN in terms of directed, effective connectivity using spDCM.

Diffusion MRI

Preprocessing. Diffusion MRI data were preprocessed through a pipeline in Functional MRI of the Brain's Diffusion Toolbox (FDT) [Smith et al., 2004], which includes skull stripping [Smith, 2002], eddy current correction, subsequent B-matrix rotation [Leemans, 2009], diffusion tensor model fitting (to obtain FA maps), and multi-fiber probabilistic diffusion model fitting [Behrens et al., 2003].

Probabilistic tractography. To estimate the probability of a tract from a given seed region, this method uses a sampling technique from distributions on voxel-wise diffusion directions. Here the seed nucleus accumbens (NAcc) mask was derived from an automated subcortical segmentation pipeline (Freesurfer) for each individual. In order to maximize reliability of the sampling procedure, 25,000 samples per voxel were drawn to generate the corresponding probabilistic map of the fronto-accumbal pathway. Tracts reaching ventricles or CSF were excluded. We then calculated a connectivity probability between the NAcc seed and each of the prefrontal target regions of interest (ROIs) by dividing the number of fiber samples reaching each target ROI by the total number of samples (25,000 $\times$ numbers of voxels within the NAcc seed mask) [Cha, 2015]. Therefore, our connectivity measures represent probabilistic connectivity that is unbiased by ROI volumes. Tractography was performed on a High Performance Computing system in the Department of Systems Biology Information Technology at Columbia University Medical Center.

Tract-based spatial statistics. Using the standard FSL TBSS procedures [Smith et al., 2006], we performed registration, resampling to 1-mm isotropic voxel size, skeletonisation (threshold: FA = 0.20), distance map calculation, and projection of the FA values onto the skeleton.

Resting-State fMRI

Preprocessing. Standard image preprocessing was performed using SPM 8 [Friston et al., 1994] and CONN toolbox [Whitfield-Gabrieli and Nieto-Castanon, 2012] for functional connectivity analysis. Slice timing correction and motion correction by linear registration to a reference image were applied. The images were coregistered with a high-resolution anatomical scan, normalized into the Montreal Neurological Institute (MNI) space, and resampled at 2 mm. Images were smoothed with a Gaussian kernel of 6 mm FWHM (full width at half maximum). In order to maximize sensitivity and specificity of resting state functional connectivity (rs-FC) measures, we considered the following confounders: in addition to the six head motion parameters estimated using linear realignment in SPM, we estimated potential artifacts (defined as frame wise displacement (FD) > 0.5 mm or signal intensity changes > 3 SD) using the artifact detection tool (ART) (https://www.nitrc.org/projects/artifact_detect); and three orthogonal time series and their derivatives from BOLD signals from white matter and cerebrospinal fluid using component-based noise-reduction approach [Behzadi et al., 2007]. These confounders were then used as nuisance regressor within the CONN Toolbox pipeline. Other signal processing in the pipeline included temporal band-pass filtering (0.008–0.09 Hz), detrending, and despiking.

Seed-based functional connectivity. Rs-FC was estimated following established methods previously described [Posner et al., 2014]. Temporal correlation (Pearson's *r*) of the resting-state BOLD time series was computed, Fisher-*z* transformed, and NAcc-seeded connectivity maps were generated [Di Martino et al., 2008].

Effective connectivity–spectral dynamic causal modeling. Based on the group difference at Session 1 in resting state fMRI within the fronto-accumbal circuit (described below), we used spDCM to further explore functional connectivity with DCM12 (revision 6080). The fMRI time series were extracted from the left NAcc using the same ROI mask for the rs-FC analysis, and the left OFC using a 6 mm radius sphere centered on the peak voxel of the rs-FC group difference results. Since These selection criteria were derived from the rs-FC analysis, the DCM analysis is supplementary, or post hoc. *Model specification*. The DCMs were constructed with bilinear connections, and with single neuronal states. We assumed all possible "endogenous" connections (A matrix in DCM terms) between the NAcc and the OFC. Thus, three different models were built and estimated across all subjects: (i) NAcc to OFC, (ii) OFC to NAcc, and (iii) reciprocal connections. *Bayesian model comparison*. Bayesian model selection computed the posterior probabilities of the competing models [Stephan et al., 2009]. Following model selection, parameters were averaged across competing models using Bayesian parameter averaging [Stephan et al., 2010].

Regions of Interest Definition

For dMRI-based tractography, seed (NAcc) and target (PFC) regions were derived from segmentation and parcellation of a high-resolution structural scan in each individual using the FreeSurfer 5.3 image analysis suite. The masks were then linearly registered to each individual's diffusion space.

Given the anatomy of the fronto-accumbal pathway described in a nonhuman primate study [Haber and Knutson, 2010], we initially estimated NAcc connectivity to the following target PFC regions: the orbitofrontal cortex (OFC; medial and lateral), anterior cingulate cortex (ACC; rostral and caudal), and dorsal PFC. Then, we selected connectivity measures with the OFC (medial and lateral) and rostral ACC ROIs for statistical analysis, while

excluded ones with the caudal ACC and dorsal PFC ROIs because they showed no meaningful connections (i.e., below a threshold of 0.02% of the total estimated streamlines, commonly used in human probabilistic tractography literature [Cha et al., 2015; Chowdhury et al., 2013; Forstmann et al., 2011]). Likewise, the subsequent voxel-wise analyses were informed by the tractography results. Thus, we used an ROI mask containing the NAcc, OFC (medial and lateral), and rostral ACC, but not the dorsal PFC and the caudal ACC; the ROIs were derived from the Harvard-Oxford cortical and subcortical atlas available in FSL (http://fsl.fmrib.ox.ac.uk/fsl/fslwiki/Atlases). The individual ROIs were merged into one mask to calculate an ROI-level threshold for multiple comparison correction. For TBSS, we used the intersection between the group mean (skeletonized) FA mask and the anatomical mask of the fronto-accumbal system.

Statistical Analysis

Overview

Across the multiple MRI measures, we used linear mixed effect (LME) models as a primary statistical model; this model accounts for covariance of repeated measures and random effects of the time variable, in addition to fixed effects.

Probabilistic tractography

LME model was performed using SPSS (IBM Inc, Chicago, IL). Each model contained the probabilistic tractography measure of each connection as the dependent variable, Diagnosis and Session as the independent variables, a Diagnosis-by-Session interaction term, and nuisance covariates (see section on "Confounding Variables"). Results were corrected for multiple testing using the false discovery rate (FDR) [Benjamini and Hochberg, 1995].

TBSS

LME model was used to examine Diagnosis-by-Session interactions. Effects of Diagnosis were examined using a separate model with averaged FA maps across sessions, because the LME model treated subject as a random effect. We controlled for multiple comparison using a cluster-extent method derived by simulation (3dClustSim program in Analysis of Functional Neuroimage [Cox, 1996]). Within a single anatomical mask of the fronto-accumbal pathway (see section on "Regions of Interest Definition"), a minimum cluster extent of 14.3 at a voxel-wise P of 0.005 was estimated under an alpha of 0.05 (based on an estimated smoothness (FWHM) of 2.46 mm and a 1 m^3 isometric voxel dimension; smoothness was estimated on a z-score map using smoothest program in FSL). For an exploratory whole brain analysis outside of our ROI, the simulation estimated a minimum cluster extent of 21.8 under the same condition. Age and the two head motion parameters (average rotation and translation) were used as nuisance covariates. GLMs were estimated using nonparametric permutation (randomize in FSL; see Supporting Information).

Resting-state functional connectivity

A general linear model was built using NAcc-seeded functional connectivity maps as the dependent variable, and Diagnosis and Subject as the independent variables in the underweight AN and HC, and nuisance covariates (see section on "Confounding Variables"). We restricted the group comparisons to the anatomical mask of the fronto-accumbal system. Statistical significance was determined with a voxel-wise threshold and cluster extent threshold, for an effective alpha of 0.05 based on Monte Carlo simulation using 3dClustSim in AFNI (Cox, 1996). Timeseries of spontaneous fMRI fluctuation was extracted using a 6 mm-radius sphere centered on the peak coordinates on both session 1 and 2 across the groups.

Confounding variables

In each statistical analysis, we first tested a full model with the nuisance covariates, such as, AN subtypes (restricting and binge eating/purging) and comorbidity, age, two in-scanner head motion estimates (see section on "Head Motion During Scanning"). After having confirmed that non-significant effects of the covariates, we reported results of the parsimonious models without the nuisance covariates. Given the sample sizes of this study, however, our full models are deemed to be underpowered in terms of detecting effects of any of the covariates.

Structural equation modeling

Bayesian SEM was used to investigate the association of structural and functional (effective) connectivity with AN. As this was a post hoc analysis, we used only Session 1 data [22 AN (15 rs-fMRI) and 18 HC (17 rs-fMRI)], as Session 1 demonstrated the most significant effects of diagnosis. We used Bayesian estimation based on MCMC sampling (100,000 iterations), which offers more reliable results for smaller samples [Lee, 2007]. As Bayesian statistics present the posterior probability of parameters that is conditional on observed data, it enables inferences about the parameters themselves. This is in contrast to a frequentist approach, which focuses on the likelihood of observing data under an assumption of fixed parameters, and therefore cannot be used to make similar claims about any individual parameters.

Two latent variables—Structural and Effective Connectivity—were estimated from the probabilistic tractography measures and DCM parameters, respectively. The two latent variables served as the predictors. Diagnosis was

used as the outcome variable. A detailed description is provided in Supporting Information.

Clinical correlates

Pearson's correlation was used to explore associations between fronto-accumbal connectivity and severity of illness among individuals with acutely-ill AN (EDE-Q global score and BMI). Significance was determined using permutation testing (100,000 iterations) and was FWE corrected for multiple comparison as described elsewhere [Groppe et al., 2011].

Head motion during scanning

We estimated average rotation and translation [Yendiki et al., 2013] for dMRI, Framewise Displacement [Power et al., 2012] and DVARS (D denoting temporal derivative of timeseries, VARS, root mean square variance over voxels) [Smyser et al., 2010]) for fMRI (see Supporting Information for group mean head motion parameters).

RESULTS

Diffusion MRI

White matter connectivity: diffusion probabilistic tractography

Probabilistic tractography successfully reconstructed fronto-accumbal white matter tracts (Fig. 1). LME models of the probabilistic connectivity measures revealed a significant effect of diagnosis on the right NAcc-right lateral OFC ($P_{FDR} = 0.006$; partial $\eta^2 = 0.384$) and the left NAcc-left lateral OFC ($P_{FDR} = 0.015$; partial $\eta^2 = 0.197$) tract measures. No significant diagnosis-by-session interactions were found (P_{FDR}'s > 0.29). *Post-hoc* analyses showed an increase in the structural connectivity measures in the underweight AN group. AN subtype, comorbidities, and in-scanner head motion had no significant effects (P's > 0.3). Change in structural connectivity was not associated with weight change (P's > 0.48) in the individuals with AN.

The effect of AN appeared specific to the NAcc-lateral OFC tract because no significant effects of diagnosis or diagnosis-by-session interaction were found in NAcc connectivity with the other ROIs (e.g., the mOFC or ACC); in an exploratory analysis, NAcc connectivity with the amygdala (potentially reflecting amygdala afferent connections to the NAcc; [Haber and Knutson, 2010], or with the midbrain ventral tegmental area (VTA, potentially reflecting the NAcc efferent connections to the VTA) (P's > 0.2; see Supporting Information Fig. 2). Non-significant effects were found on the total numbers of NAcc-seeded tracts (streamlines) (P's > 0.6). Furthermore, the increased NAcc-lOFC structural connectivity was not attributable to an abnormal seed or target region because non-significant effects were found in the NAcc volumes or thickness of the lateral OFC.

White matter integrity: tract-based spatial statistics

We tested whether AN is associated with abnormal white matter integrity within the fronto-accumbal pathway. Compared with HC, participants with AN showed significantly increased FA before and after weight restoration in the white matter near the lateral OFC and the NAcc ($P_{ROI} < 0.03$; peak $P = 0.000036$, MNI xyz = −24 10 −13, cluster extent = 16 voxels; ROI analysis within the fronto-accumbal white matter; Figure 1; see Supporting Information Figure 3 for exploratory whole brain analysis). We found no significant effect of session or diagnosis-by-session interaction (P's > 0.2). Mean FA of the whole brain white matter did not significantly differ between the groups ($P > 0.7$). AN subtype, comorbidities, and in-scanner head motion had no significant effects on the fronto-accumbal FA (P's > 0.7).

Resting-State MRI

Voxel-wise seed-based functional connectivity

Voxel-wise analysis showed increased functional connectivity of the left NAcc-left medial OFC in underweight participants with AN compared with HC ($P_{FWE\ ROI} < 0.01$; Fig. 2). LME models based on this cluster revealed a significant effect of diagnosis ($P_{FDR} = 0.032$; functional connectivity estimates extracted from the cluster in both sessions). Effects of AN subtypes were non-significant ($P > 0.1$). Within this OFC cluster, a significant interaction of diagnosis-by-session was observed ($P < 0.009$); however, this was driven largely by a significant change in connectivity in the HC (Session 1–Session 2: $t = -2.07$, $P < 0.046$) rather than AN ($t = 1.71$, $P > 0.096$). AN subtype, comorbidities, and in-scanner head motion had no significant effects on the tract measures (P's > 0.4).

Effective connectivity: spectral dynamic causal modeling

Out of three DCMs estimated (Fig. 3A), Bayesian model selection showed the highest expected probability and exceedance probability for the model with an excitatory "top-down" influence from the OFC to NAcc (Fig. 3B; positive connectivity in DCM represents an excitatory connection; negative represents inhibitory). Bayesian parameter averaging on all three models revealed non-significant group differences in effective connectivity (P's > 0.3). Bayesian parameter averaging also showed that the "top-down" excitatory OFC-to-NAcc influence was two-fold greater than the "bottom-up" NAcc-to-OFC influence ($P < 0.05$; Wilcoxon signed rank test) (Fig. 3C).

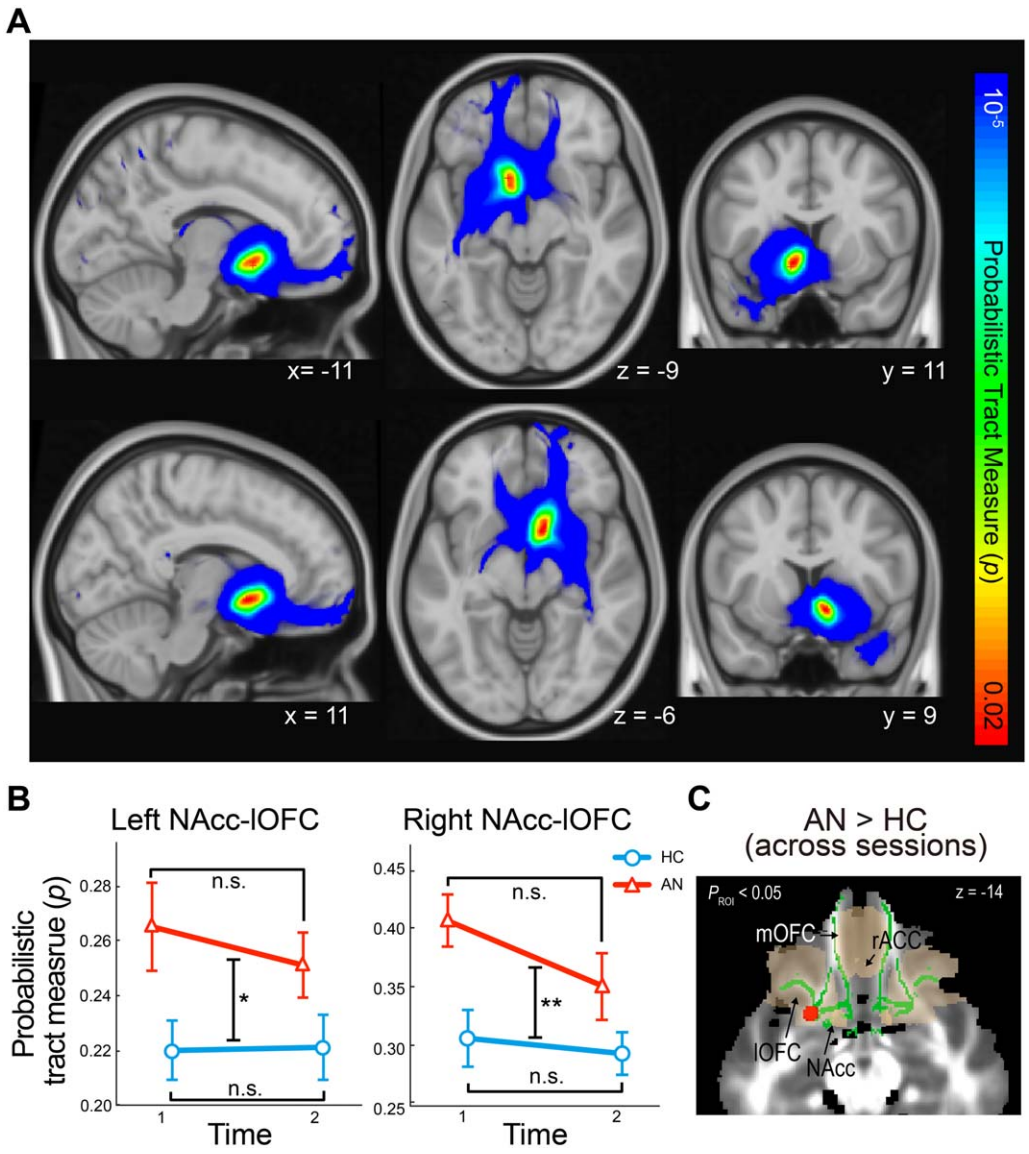

Figure 1.

Abnormal fronto-accumbal structural connectivity in anorexia nervosa. (A) Successfully reconstructed fronto-accumbal white matter tracts using diffusion MRI-probabilistic tractography (top row, the left NAcc seeded tracts; bottom, the right NAcc seeded tracts). (B) Individuals with AN showed greater structural connectivity before and after weight restoration within the left and right NAcc-OFC connections compared with healthy controls ($P_{FWE} < 0.05$). (C) Greater fractional anisotropy in AN compared with healthy controls before and after weight restoration (shown in red) within the fronto-accumbal white matter Region of Interest (shown in green). Error bars indicate sem. * $P < 0.05$; ** $P < 0.01$. n.s., non-significant. AN, anorexia nervosa; HC, healthy controls; lOFC, lateral orbitofrontal cortex; NAcc, nucleus accumbens; rACC, rostral anterior cingulate cortex.

Structural Equation Modeling

We further explored the relationship between fronto-accumbal connectivity and AN using multivariate SEM. We excluded Session 2 data from the SEM because of the significant difference in rs-FC in HC across sessions. Our model confirmed that increased fronto-accumbal structural connectivity (i.e., a latent variable estimated from the diffusion tractography measures) was significantly associated with underweight AN. We also observed that decreased fronto-accumbal effective connectivity (the other latent variable, estimated from spDCM parameters) was associated with underweight AN (Fig. 4). At the observed variable level, a stronger inhibitory OFC-to-OFC connection

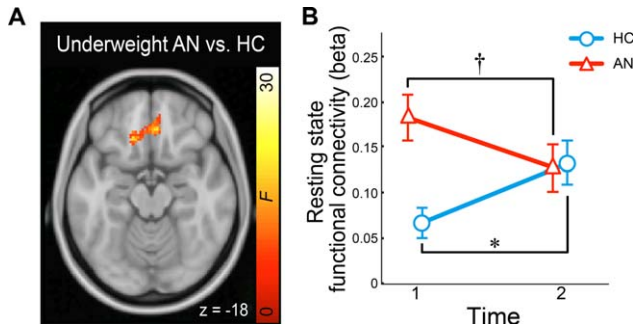

Figure 2.

Abnormal fronto-accumbal resting state functional connectivity in anorexia nervosa (AN). (A) Group differences in NAcc-seeded functional connectivity are shown (*F*-contrast of underweight AN vs. healthy controls, HC). (B) NAcc-OFC functional connectivity before and after weight restoration in AN compared with HC (a linear mixed effect model). * $P < 0.05$, † $P < 0.01$. Error bars denote one sem.

(i.e., a greater negative value) and a weaker excitatory OFC-to-NAcc connection (i.e., a smaller positive value) contributed to more atypical effective connectivity in AN. The two latent variables (structural and effective connectivity) showed a modest covariance (posterior probability = 0.855). The model showed a good model fit with a posterior predictive probability of 0.50 [Gelman et al., 1996].

Clinical Correlates

There was a significant correlation between the right NAcc-lateral OFC structural connectivity and the EDE-Q at Session 1 among the individuals with AN (Pearson's $r = 0.463$, $P_{FWE} = 0.041$; controlled for multiple comparison; Fig. 5). The other connectivity estimates showed no significant correlations (P_{FWE}'s > 0.29).

Individuals with AN showed significant improvement in symptom severity with weight restoration, as shown in Table I (EDE-Q: $t = 3.604$, $P = 0.009$; paired t test, two-tailed). No significant correlations were found between changes in the connectivity estimates and improvement in EDE-Q (P's > 0.7; Fig. 5).

DISCUSSION

This longitudinal study examined the fronto-accumbal pathway in AN using multimodal MRI. We found that within the fronto-accumbal pathway, underweight individuals with AN had increased structural connectivity, increased white matter anisotropy, increased functional connectivity, and altered effective connectivity (decreased OFC-to-NAcc excitation and increased recurrent OFC inhibition connections). The increased fronto-accumbal structural connectivity in the underweight state persisted following weight restoration and was associated with a measure of eating disorder severity. These findings suggest that hyperconnectivity in reward circuitry may be an important neural substrate in AN.

Prior diffusion MRI research in AN has reported decreased white matter integrity (either decreased FA or increased MD) in white matter regions near the hippocampus [Kazlouski et al., 2011], the occipital gyrus [Via et al., 2014], and the cerebellum [Nagahara et al., 2014]. However, white matter within the fronto-accumbal system has rarely

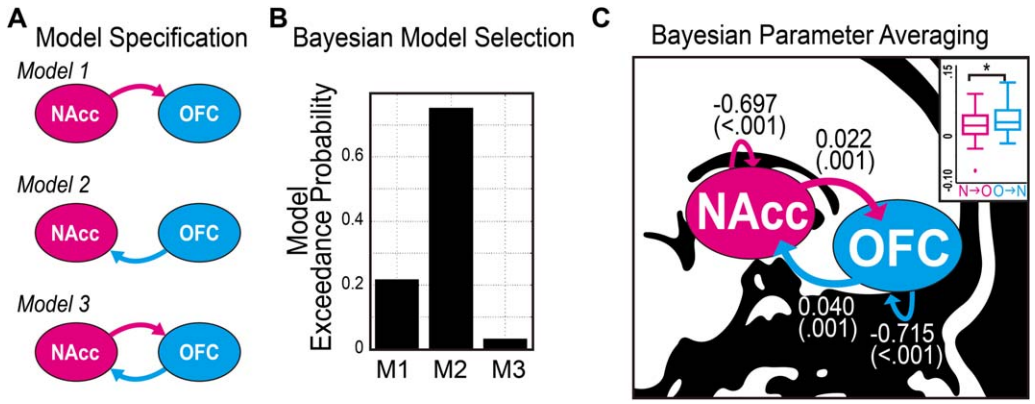

Figure 3.

Fronto-accumbal effective connectivity estimated by spectral dynamic causal model (DCM). (A) Bayesian model specification for spectral DCM. (B) In the random effect Bayesian model selection scheme, Model 2 showed the highest model exceedance probability. (C) Bayesian Parameter Averaging using all three models showed significant bilateral excitatory connections between the OFC and the NAcc, and inhibitory recurrent connections. Connectivity estimates were shown (in Hertz) with *P* values to be different from zero (non-parametric Wilcoxon signed rank test). As shown in the boxplot, the OFC to NAcc connectivity was greater than the NAcc to OFC connectivity (Wilcoxon signed rank test). NAcc, nucleus accumbens; OFC, orbitofrontal cortex. *$P < 0.05$. [Color figure can be viewed at wileyonlinelibrary.com]

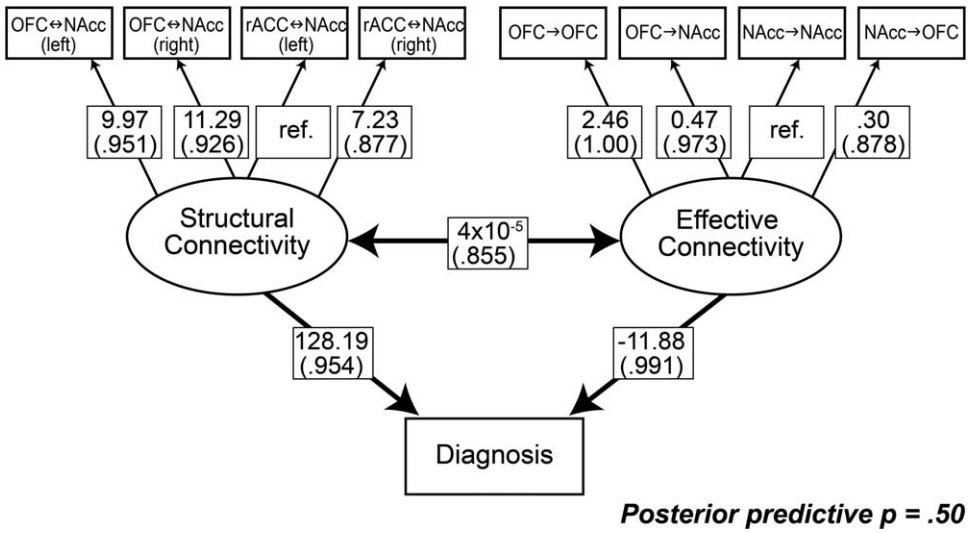

Figure 4.

Structural equation modeling revealed significant effects of effective connectivity and structural connectivity of the fronto-accumbal circuit on diagnosis. SEM was estimated using a Bayesian approach based on Markov Chain Monte Carlo sampling (100,000 iterations). Only Session 1 data [22 AN (15 resting state fMRI) and 18 HC (17 resting state fMRI)] were included in this model, for the functional connectivity showed a reliability issue across session in HC (see section on "Results"). Model parameters are provided with posterior probabilities for regression weights or covariance to be different from zero (in parenthesis). Ref denotes reference weights to enable parameter estimation.

been reported in AN. Moreover, prior DTI studies of AN have relied largely upon a single methodology (i.e., TBSS) to examine microstructure of the white matter. Our study adds to the growing literature on the white matter in AN by offering multifaceted evidence of hyperconnectivity within the fronto-accumbal system across MRI modalities (diffusion and resting state functional MRI), imaging analytic techniques (tractography, TBSS, functional connectivity, and spDCM), and statistical approaches (univariate and multivariate). In addition, the fronto-accumbal hyperconnectivity in AN appears specific to the white matter tracts connecting the NAcc with the bilateral lateral OFC for the following reasons: no significant effects of AN were observed on the NAcc connections with other prefrontal ROIs or with the amygdala or midbrain ventral tegmental area (putative efferent projections of the NAcc), on the total NAcc-seeded fiber counts, or on other gray matter morphometric measures of the ROIs (the NAcc and PFC).

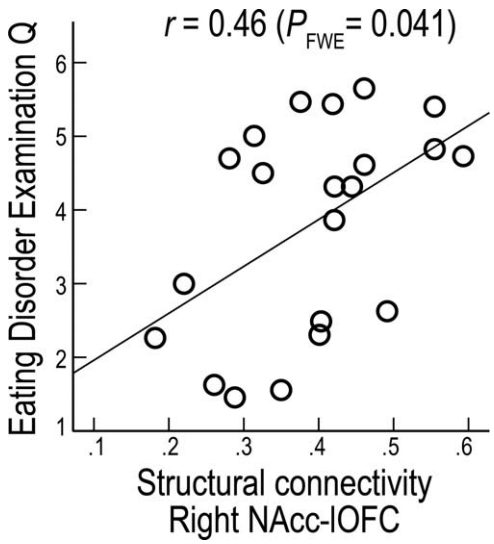

Figure 5.

Correlation between fronto-accumbal structural connectivity and eating disorder severity in AN. In individuals with AN, Right NAcc-lateral OFC baseline structural connectivity was correlated with EDE-Q [Pearson's correlation; significance was controlled for multiple comparison using family-wise error (FWE) rate via permutation testing].

Our DCM and SEM results have implications about the pathophysiology of AN, as well as for methodological approaches to studying AN. First, the best model in Bayesian Model Selection [Stephan et al., 2010] features the "top-down" OFC-to-NAcc excitatory connection. This excitatory connection is in line with the major afferent pathway of the ventral striatum coming from the ventral frontal regions [Haber and Knutson, 2010]. Of note, this Bayesian model comparison shows the same best model for both healthy individuals and those acutely ill with AN, suggesting a common underlying model structure in both groups within the fronto-accumbal resting-state functional circuit. Second, whereas a univariate approach failed to show group differences in effective connectivity estimates,

a multivariate approach (e.g., SEM) showed strong evidence for an association between underweight AN and abnormal fronto-accumbal effective connectivity: a decrease in the OFC-to-NAcc excitatory connection and an increase in the OFC recurrent inhibitory connection. The divergence of univariate vs. multivariate findings suggests that, whereas individual connections may not be significantly altered in AN, the pattern of fronto-accumbal connections may be informative. This underscores the potential importance of multivariate approaches to neuroimaging research in psychiatry. Third, the SEM results indicate that the recurrent OFC (i.e., OFC-to-OFC) inhibitory connection may be the fronto-accumbal connection most affected in AN. This suggests a potential area for future research, that is, an altered inhibitory tone (i.e., Gamma-aminobutyric acid or GABA transmission) in the OFC in AN.

The persistence of the heightened structural connectivity in AN even after weight restoration may relate to the remarkable persistence of this disorder: for example, up to 50% of affected individuals require rehospitalization within a year of discharge [Pike, 1998]. It is possible that increased structural connectivity of the fronto-accumbal reward pathway is related to the persistence of AN, potentially via interplay with basal ganglia *habit* circuitry [Walsh, 2013]. Interaction between these two circuitries has been well documented: reward encoding plays a pivotal role in habit formation [Barnes et al., 2005]. In AN, abnormal reward processing within reward circuitry (e.g., the fronto-accumbal pathway) may interact dynamically with abnormal habit learning within the habit circuitry (e.g., the basal ganglia-dorsal PFC pathway). Future investigation on the interaction of the two circuits and how this relates to the course of the disorder may be of great interest. Future research might also consider the behavioral consequences of altering fronto-accumbal hyperconnectivity using, for example, pharmacological probes and/or brain stimulation techniques.

Study limitations are worth noting. First, our report is based on a 1.5 T MRI scanner, which has a lower signal-to-noise ratio than 3 T or higher field magnets. An increase in magnetization power may improve the sensitivity and specificity of connectivity measures. Second, we used 16 non-collinear directions of diffusion weighting. Although increasing the diffusion directions may improve the accuracy of tractography, however, a recent comparison study indicates that the reproducibility (within-subject, inter-session) of probabilistic tractography does not differ in 12 versus 60 direction dMRI [Heiervang et al., 2006]. Lastly, the current findings need to be considered in light of the small sample size and the need for replication.

CONCLUSION

This longitudinal study provides convergent evidence of atypical connectivity within the fronto-accumbal circuit in AN. It further shows that this atypical connectivity may not fully resolve with weight restoration. Further research is needed to evaluate whether this circuit eventually normalizes with maintenance of healthy eating and weight, or persists even after remission of illness. Remaining to be tested in future studies across sites and across patient samples are: generalizability of our findings, clinical utility of the MR-based connectivity estimates of the fronto-accumbal pathway (e.g., as predictive measures for treatment response), and, ultimately, the role of the fronto-accumbal circuit in the neural mechanisms of AN.

ACKNOWLEDGMENT

The authors thank Dr. Dominik Biezonski for insightful discussion.

REFERENCES

Arcelus J, Mitchell AJ, Wales J, Nielsen S (2011): Mortality rates in patients with anorexia nervosa and other eating disorders. A meta-analysis of 36 studies. Arch Gen Psychiatry 68:724–731.

Attia E, Walsh BT (2009): Behavioral management for anorexia nervosa. N Engl J Med 360:500–506.

Barnes TD, Kubota Y, Hu D, Jin DZ, Graybiel AM (2005): Activity of striatal neurons reflects dynamic encoding and recoding of procedural memories. Nature 437:1158–1161.

Behrens TE, Woolrich MW, Jenkinson M, Johansen-Berg H, Nunes RG, Clare S, Matthews PM, Brady JM, Smith SM (2003): Characterization and propagation of uncertainty in diffusion-weighted MR imaging. Magn Reson Med 50:1077–1088.

Behzadi Y, Restom K, Liau J, Liu TT (2007): A component based noise correction method (CompCor) for BOLD and perfusion based fMRI. Neuroimage 37:90–101.

Benjamini Y, Hochberg Y (1995): Controlling the false discovery rate: A practical and powerful approach to multiple testing. J R Stat Soc Ser B (Methodological) 57:289–300.

Broft A, Slifstein M, Osborne J, Kothari P, Morim S, Shingleton R, Kenney L, Vallabhajosula S, Attia E, Martinez D, Timothy Walsh B (2015): Striatal dopamine type 2 receptor availability in anorexia nervosa. Psychiatry Res 233:380–387.

Cha J, Fekete T, Siciliano F, Biezonski D, Greenhill L, Pliszka SR, Blader JC, Roy AK, Leibenluft E, Posner J (2015): Neural correlates of aggression in medication naive children with ADHD: Multivariate analysis of morphometry and tractography. Neuropsychopharmacology 40:1717–1725.

Chowdhury R, Guitart-Masip M, Lambert C, Dayan P, Huys Q, Düzel E, Dolan RJ (2013): Dopamine restores reward prediction errors in old age. Nat Neurosci 16:648–653.

Cooper Z, Fairburn C (1987): The eating disorder examination A semi-structured interview for the assessment of the specific psychopathology of eating disorders. Int J Eat Disord 6:1–8.

Cowdrey FA, Park RJ, Harmer CJ, McCabe C (2011): Increased neural processing of rewarding and aversive food stimuli in recovered anorexia nervosa. Biol Psychiatry 70:736–743.

Cox RW (1996): AFNI: Software for analysis and visualization of functional magnetic resonance neuroimages. Comput Biomed Res 29:162–173.

Decker JH, Figner B, Steinglass JE (2015): On weight and waiting: Delay discounting in anorexia nervosa pretreatment and posttreatment. Biol Psychiatry 78:606–614.

Di Martino A, Scheres A, Margulies D, Kelly A, Uddin L, Shehzad Z, Biswal B, Walters J, Castellanos F, Milham M (2008): Functional connectivity of human striatum: A resting state FMRI study. Cerebr Cortex 18:2735.

Fairburn CG, Beglin SJ (1994): Assessment of eating disorders: Interview or self-report questionnaire? Int J Eat Disord 16: 363–370.

Fladung AK, Gron G, Grammer K, Herrnberger B, Schilly E, Grasteit S, Wolf RC, Walter H, von Wietersheim J (2010): A neural signature of anorexia nervosa in the ventral striatal reward system. Am J Psychiatry 167:206–212.

Forstmann BU, Tittgemeyer M, Wagenmakers EJ, Derrfuss J, Imperati D, Brown S (2011): The speed-accuracy tradeoff in the elderly brain: A structural model-based approach. J Neurosci 31:17242–17249.

Frank GK, Bailer UF, Henry SE, Drevets W, Meltzer CC, Price JC, Mathis CA, Wagner A, Hoge J, Ziolko S (2005): Increased dopamine D2/D3 receptor binding after recovery from anorexia nervosa measured by positron emission tomography and [< sup> 11 C] raclopride. Biol Psychiatry 58:908–912.

Frank GK, Shott ME, Hagman JO, Mittal VA (2013a): Alterations in brain structures related to taste reward circuitry in ill and recovered anorexia nervosa and in bulimia nervosa. Am J Psychiatry 170:1152–1160.

Friston KJ, Holmes AP, Worsley KJ, Poline JP, Frith CD, Frackowiak RS (1994): Statistical parametric maps in functional imaging: A general linear approach. Hum Brain Mapp 2: 189–210.

Gelman A, Meng XL, Stern H (1996): Posterior predictive assessment of model fitness via realized discrepancies. Stat Sinica 6: 733–760.

Goodman WK, Price LH, Rasmussen SA, Mazure C, Delgado P, Heninger GR, Charney DS (1989): The yale-brown obsessive compulsive scale: II. Validity. Arch Gen Psychiatry 46:1012.

Graybiel AM, Rauch SL (2000): Toward a neurobiology of obsessive-compulsive disorder. Neuron 28:343–347.

Groppe DM, Urbach TP, Kutas M (2011): Mass univariate analysis of event-related brain potentials/fields II: Simulation studies. Psychophysiology 48:1726–1737.

Haber SN, Knutson B (2010): The reward circuit: Linking primate anatomy and human imaging. Neuropsychopharmacology 35: 4–26.

Heiervang E, Behrens TE, Mackay CE, Robson MD, Johansen-Berg H (2006): Between session reproducibility and between subject variability of diffusion MR and tractography measures. Neuroimage 33:867–877.

Hudson JI, Hiripi E, Pope HG, Kessler RC (2007): The prevalence and correlates of eating disorders in the National Comorbidity Survey Replication. Biol Psychiatry 61:348–358.

Insel TR (2009): Disruptive insights in psychiatry: Transforming a clinical discipline. J Clin Investig 119:700–705.

Kaye WH, Fudge JL, Paulus M (2009): New insights into symptoms and neurocircuit function of anorexia nervosa. Nat Rev Neurosci 10:573–584.

Kazlouski D, Rollin MD, Tregellas J, Shott ME, Jappe LM, Hagman JO, Pryor T, Yang TT, Frank GK (2011): Altered fimbria-fornix white matter integrity in anorexia nervosa predicts harm avoidance. Psychiatry Res 192:109–116.

Lee S-Y (2007): Structural Equation Modeling; A Bayesian Approach. Hoboken, N.J.: John Wiley & Sons. 432 p.

Leemans A (2009): The -matrix must be rotated when correcting for subject motion in DTI data. Magn Reson Med 61:1336–1349.

Mori S, Zhang J (2006): Principles of diffusion tensor imaging and its applications to basic neuroscience research. Neuron 51: 527–539.

Nagahara Y, Nakamae T, Nishizawa S, Mizuhara Y, Moritoki Y, Wada Y, Sakai Y, Yamashita T, Narumoto J, Miyata J, Yamada K, Fukui K (2014): A tract-based spatial statistics study in anorexia nervosa: Abnormality in the fornix and the cerebellum. Prog Neuropsychopharmacol Biol Psychiatry 51:72–77.

O'Hara CB, Campbell IC, Schmidt U (2015): A reward-centred model of anorexia nervosa: A focussed narrative review of the neurological and psychophysiological literature. Neurosci Biobehav Rev 52:131–152.

Pike KM (1998): Long-term course of anorexia nervosa: Response, relapse, remission, and recovery. Clin Psychol Rev 18:447–475.

Posner J, Marsh R, Maia TV, Peterson BS, Gruber A, Simpson HB (2014): Reduced functional connectivity within the limbic cortico-striato-thalamo-cortical loop in unmedicated adults with obsessive-compulsive disorder. Hum Brain Mapp 35: 2852–2860.

Power JD, Barnes KA, Snyder AZ, Schlaggar BL, Petersen SE (2012): Spurious but systematic correlations in functional connectivity MRI networks arise from subject motion. Neuroimage 59:2142–2154.

Razi A, Kahan J, Rees G, Friston KJ (2015): Construct validation of a DCM for resting state fMRI. NeuroImage 106:1–14.

Smith SM (2002): Fast robust automated brain extraction. Hum Brain Mapp 17:143–155.

Smith SM, Jenkinson M, Woolrich MW, Beckmann CF, Behrens TE, Johansen-Berg H, Bannister PR, De Luca M, Drobnjak I, Flitney DE (2004): Advances in functional and structural MR image analysis and implementation as FSL. NeuroImage 23:S208–S219.

Smith SM, Jenkinson M, Johansen-Berg H, Rueckert D, Nichols TE, Mackay CE, Watkins KE, Ciccarelli O, Cader MZ, Matthews PM, Behrens TEJ (2006): Tract-based spatial statistics: Voxelwise analysis of multi-subject diffusion data. Neuroimage 31:1487–1505.

Smyser CD, Inder TE, Shimony JS, Hill JE, Degnan AJ, Snyder AZ, Neil JJ (2010): Longitudinal analysis of neural network development in preterm infants. Cerebr Cortex 20: 2852–2862.

Stephan KE, Penny WD, Daunizeau J, Moran RJ, Friston KJ (2009): Bayesian model selection for group studies. Neuroimage 46: 1004–1017.

Stephan KE, Penny WD, Moran RJ, den Ouden HE, Daunizeau J, Friston KJ (2010): Ten simple rules for dynamic causal modeling. Neuroimage 49:3099–3109.

Titova OE, Hjorth OC, Schiöth HB, Brooks SJ (2013): Anorexia nervosa is linked to reduced brain structure in reward and somatosensory regions: A meta-analysis of VBM studies. BMC Psychiatry 13:110.

Via E, Zalesky A, Sanchez I, Forcano L, Harrison BJ, Pujol J, Fernandez-Aranda F, Menchon JM, Soriano-Mas C, Cardoner N, Fornito A (2014): Disruption of brain white matter microstructure in women with anorexia nervosa. J Psychiatry Neurosci 39:367–375.

Wagner A, Aizenstein H, Venkatraman VK, Fudge J, May JC, Mazurkewicz L, Frank GK, Bailer UF, Fischer L, Nguyen V, Carter C, Putnam K, Kaye WH (2007): Altered reward

processing in women recovered from anorexia nervosa. Am J Psychiatry 164:1842–1849.
Walsh BT (2013): The enigmatic persistence of anorexia nervosa. Am J Psychiatry 170:477–484.
Wechsler D (2001): Wechsler Test of Adult Reading: WTAR. San Antonio: Tex. Psychological Corp. Test
Whitfield-Gabrieli S, Nieto-Castanon A (2012): Conn: A functional connectivity toolbox for correlated and anticorrelated brain networks. Brain Connect 2:125–141.
Yendiki A, Koldewyn K, Kakunoori S, Kanwisher N, Fischl B (2013): Spurious group differences due to head motion in a diffusion MRI study. Neuroimage 88C:79–90.